Transition Metal Chemistry of Main Group Hydrazides. 11.[1] Synthesis and Coordination Chemistry of Novel Tetraphosphano Phosphorinanes. X-ray Crystal Structure of $[\{W(CO)_4\}_2\{\mu\text{-}[PhPN(Me)N(P(OCH_2CF_3)_2)]_2\}]$

V. Sreenivasa Reddy,[†] Kattesh V. Katti,*[,†] and Charles L. Barnes[‡]

Center for Radiological Research and MU Research Reactor, Allton Building Laboratories, 301 Business Loop 70 West, Columbia, Missouri 65203, and Department of Chemistry, University of Missouri, Columbia, Missouri 65211

Received July 28, 1994

Introduction

The use of alkane diphosphines ($R_2P(CH_2)_nPR_2$; $n = 1-3$) as chelating ligands has been widely exploited, but only recently has attention turned toward the development of a new generation of chelating phosphines bridged by non-carbon centers. The incorporation of hetero atoms such as oxygen, sulfur and nitrogen bridging the two phosphines (eg., $(R_2P-E-PR_2$; E = O, S, or NR′) have been explored. However, the discovery of bis(dihalophosphino)amines ($Cl_2P-N(R)-PCl_2$) has resulted in the development of a large number of functionalized bis(phosphino)amines of general formula **A**.[2−16] To date, more than 300 papers have been published describing the rich coordination chemistry of cyclic and acylic $R_2P-N(R')-PR_2$-based ligand frameworks.[2−16] While the synthetic versatility and the structural diversity of bis(phosphino)amine ligands and their metal complexes continue to demonstrate the importance of non-carbon-bridged diphosphines, a major discrepancy is concerned with the lack of chemical flexibility of the >P−N(R)−P< backbone. Toward this endeavor, we have recently reported novel and rational synthetic strategies to the cyclic and acyclic >P−N(R)−N(R)−P<-based dinitrogen bridged diphosphines.[17−19] The dinitrogen-bridged diphosphines of the general formula **B** may be regarded as the next homologues to the bis(phosphino)amines **A**. Our recent studies on the coordination chemistry of >P−N(R)−N(R)−P<-based ligands demonstrate the vast potential for the development of the transition metal chemistry of this new generation of chelating bis(phosphines).[18,19]

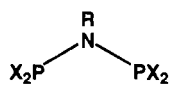

A

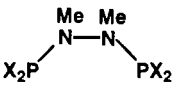

B

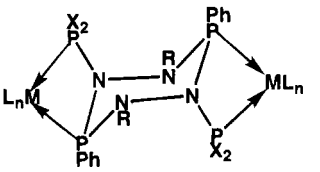

C

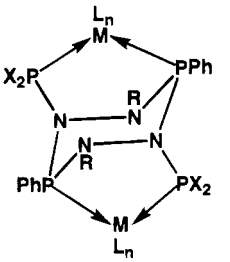

D

New main group compounds which can combine the reactivities of >P−N(R)−P< and also >P−N(R)−N(R)−P< frameworks in a single compound *via* a tetraphosphane network are important in the context of studying the coordination chemistry of multiphosphine ligands. The coordination chemistry of such multifunctional phosphanes may offer an important insight on the preferred mode of coordinations (viz., **C** vs **D**) and also provide unique opportunities for the construction of new bi- and multimetallic organometallic compounds. Herein, we report the first example of a novel tetraphosphane which contains both >P−N−P< and >P−N−N−P< functionalities in a cyclic network. The fundamental coordination chemistry of this new class of ligands is discussed in terms of its reactions with the group 6 transition metal carbonyl precursors and also through an X-ray crystal structure of a W(0) representative.

Results and Discussion

The heterocyclic phosphorinane $[PhPN(Me)N(H)]_2$ used as a synthon in the present investigation was recently synthesized in our laboratory.[17] The reaction of PPh_2Cl with 1,2,4,5-tetraza-3,6-diphosphorinane $[PhPN(Me)N(H)]_2$ (**1**) in the presence of Et_3N at 25 °C affords the new heterocyclic phosphorinane, $[PhPN(Me)N(PPh_2)]_2$ (**2**) in 84% yield (Scheme 1).[17,20] The alkoxy derivative, $[PhPN(Me)N(P(OCH_2CF_3)_2)]_2$ (**4**), was synthesized, first by the treatment of PCl_3 with **1** in the presence of Et_3N to produce the intermediate $[PhPN(Me)N(PCl_2)]_2$ (**3**), followed by the treatment of CF_3CH_2OH (Scheme 2). Compounds **2**−**4** are the first examples of main group heterocyclics which combine the phosphinoamine (>P−N−P<) and phos-

[†] Center for Radiological Research and MU Research Reactor, Allton Building Laboratories.

[‡] Department of Chemistry, University of Missouri.

(1) Part 10: Pandurangi, R. S.; Kuntz, R. R.; Volkert, W. A.; Barnes, C. L.; Katti, K. V. *J. Chem. Soc., Dalton Trans.*, in press.
(2) Nixon, J. F. *J. Chem. Soc. A* **1968**, 2689.
(3) Davies, A. R.; Dronsfield, A. T.; Haszeldine, R. N.; Taylor, D. R. *J. Chem. Soc.*, Perkin Trans. *1* **1973**, 379.
(4) Jefferson, R.; Nixon, J. F.; Painter, T. M.; Keat, R.; Stobbs, L. *J. Chem. Soc., Dalton Trans.* **1973**, 1414.
(5) For leading reviews in this area see: (a) Balakrishna, M. S.; Reddy, V. S.; Krishnamurthy, S. S.; Burckett St. Laurent, J. C. T. R.; Nixon, J. F. *Coord. Chem. Rev.* **1993**, *124*, 1. (b) King, R. B. *Acc. Chem. Res.* **1980**, *13*, 243.
(6) Field, J. S.; Haines, R. J.; Sundermeyer, J.; Woollam, S. F. *J. Chem. Soc., Dalton Trans.* **1993**, 2735.
(7) Cotton, F. A.; Ilsley, W. H.; Kaim, W. *J. Am. Chem. Soc.* **1980**, *102*, 1918.
(8) Field, J. S.; Haines, R. J.; Jay, J. A. *J. Organomet. Chem.* **1978**, *100*, 236.
(9) Derringer, D. R.; Fanwick, P. E.; Moran, J.; Walton, R. A. *Inorg. Chem.* **1989**, *28*, 1384.
(10) Dulebohn, J. I.; Ward, D. L.; Nocera, D. G. *J. Am. Chem. Soc.* **1990**, *112*, 2969.
(11) Ellermann, J.; Knoch, F. A.; Meier, K. J. *Z. Naturforsch.* **1990**, *45B*, 1657.
(12) Dumond, D. S.; Richmond, M. G. *J. Am. Chem. Soc.* **1988**, *100*, 7547.
(13) Tarassoli, A.; Chen, H.-J.; Thompson, M. L.; Allured, U. S.; Haltiwanger, R. C.; Norman, A. D. *Inorg. Chem.* **1986**, *25*, 4152.
(14) Fischer, E. O.; Keller, W.; Gasser, B. Z.; Schubert, U. *J. Organomet. Chem.* **1980**, *199*, C24.
(15) (a) Mague, J. T.; Johnson, M. P. *Organometallics*, **1990**, *9*, 1254. (b) Mague, J. T.; Lin, Z. *Organometallics*, **1992**, *11*, 4139.
(16) (a) Reddy, V. S. Transition Metal Organometallic Chemistry of $1,3,2\lambda^3,4\lambda^3$-Diazadiphosphetidines. Ph.D. Thesis, Indian Institute of Science, 1992. (b) Kamalesh Babu, R. P.; Krishnamurthy, S. S.; Nethaji, M. *J. Organomet. Chem.* **1993**, *454*, 157.
(17) Reddy, V. S.; Katti, K. V.; Barnes, C. L. *Chem. Ber.* **1994**, *127*, 979.
(18) Reddy, V. S.; Katti, K. V. *Inorg. Chem.* **1994**, *33*, 2695.
(19) Reddy, V. S.; Katti, K. V.; Barnes, C. L. *Chem. Ber.* **1994**, *127*, 1355.
(20) IUPAC name for compounds **2**−**4**: 1,4-diphosphano-1,2,4,5,$3\lambda^3$,$6\lambda^3$-tetraazadiphorinanes.

0020-1669/95/1334-1273$09.00/0

Scheme 1

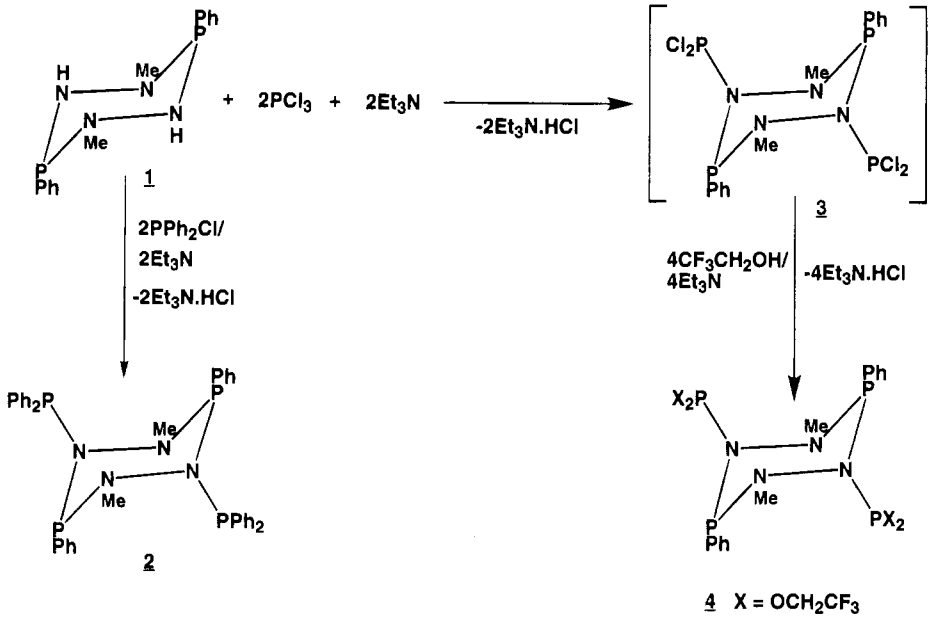

Scheme 2

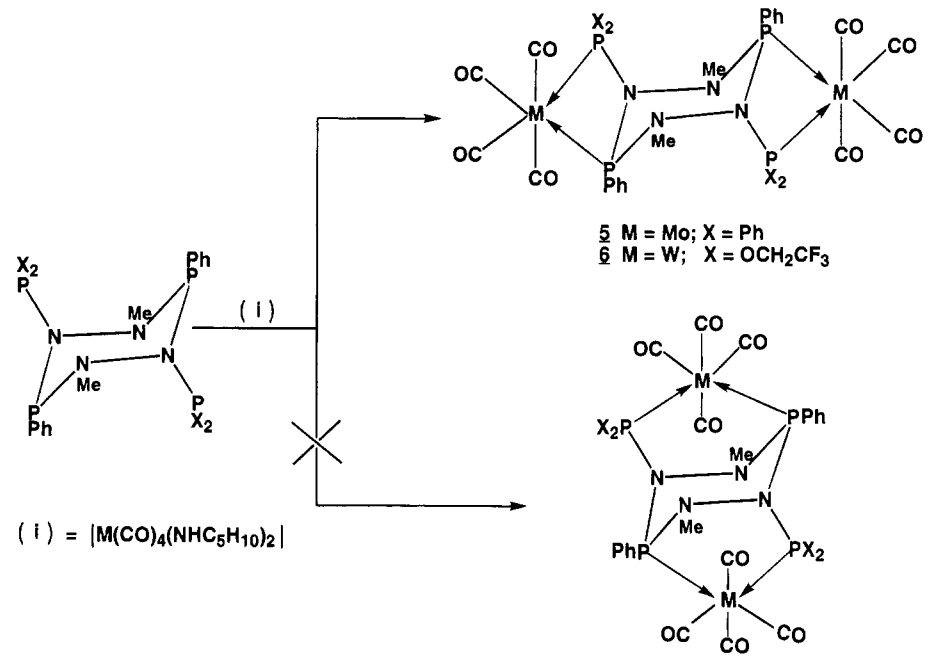

phorus hydrazide (>P−N−N−P<) functionalities in a novel tetraphosphane framework. The new tetraphos ligands **2** and **4** are air stable, white crystalline solids. The chemical constitutions of **2** and **4** were established by C, H, and N analytical data.

The formation of these phosphorinanes, **2**−**4**, is evident from the $[AX]_2$ spin pattern in their ^{31}P NMR spectra. The ^{31}P NMR spectrum of **2** showed two doublets centered at δ 64.6 ($^2J_{P-P}$ = 31.2 Hz) and δ 106.2 ($^2J_{P-P}$ = 31.2 Hz) attributed to the $-PPh_2$ and >PPh functionalities respectively. The remarkable deshielding of the >PPh chemical shift in **2** as compared to that observed in the parent precursor **1** (δ for >PPh = 89.2) is of note. The intermediate compound **3** was not isolated, however, its ^{31}P NMR spectrum consisted of two doublets centered at δ 167.3 ($^2J_{P-P}$ = 40.2 Hz, attributed to $-PCl_2$) and at δ 87.4 ($^2J_{P-P}$ = 40.2 Hz; attributed to >PPh) support the proposed composition (Scheme 1). The chemical shift of >PPh groups in **4** (δ 85.1) showed only a modest difference from that found in **3**; however, part of the AX doublet centered at δ 147.5 ($^2J_{P-P}$ = 37.0 Hz) indicated the transformation of the $>PCl_2$ group of **3** to $-P(OCH_2CF_3)_2$ in **4**. The ^1H NMR spectra of **2**−**4** are consistent with the formulations proposed in Scheme 1.

Coordination Chemistry of Tetraphosphane Ligands. The tetradentate ligand **2** reacted smoothly with 2 molar equiv of *cis*-$[Mo(CO)_4(NHC_5H_{10})_2]$, to give the dinuclear complex $[\{Mo(CO)_4\}_2\{\mu$-[PhPN(Me)N(PPh$_2$)]$_2$] (**5**) in 72% yield. Similarly, the reaction of **4** with *cis*-$[W(CO)_4(NHC_5H_{10})_2]$ affords the analogous dinuclear complex **6** in 65% yield (Scheme 2). The chemical constitutions of **5** and **6** were confirmed by analytical data. The disposition of the carbonyl groups in the octahedral complexes **5** and **6** is *cis* as confirmed by IR spectroscopy (ν(CO for **5**, 2022(sh), 1954(s), 1923(m), 1894(vs) cm^{-1}; (ν(CO) for **6**, 2037(sh), 1957(m), and 1925(s, br)). The ^{31}P NMR spectrum of **5** consisted of an $[AX]_2$ spin pattern with doublets centered at 97.4 ($^2J_{P-P}$ = 45.0 Hz) and 121.0 ppm, attributed

Scheme 3

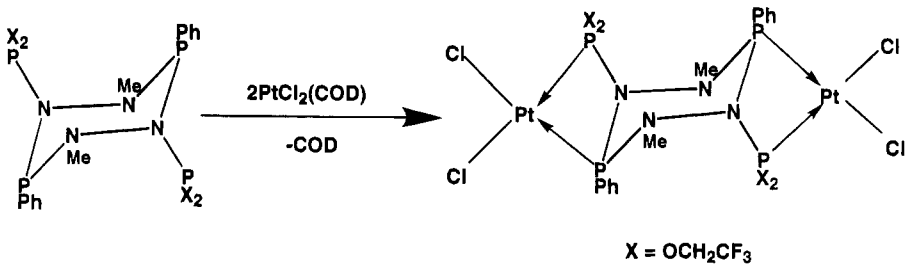

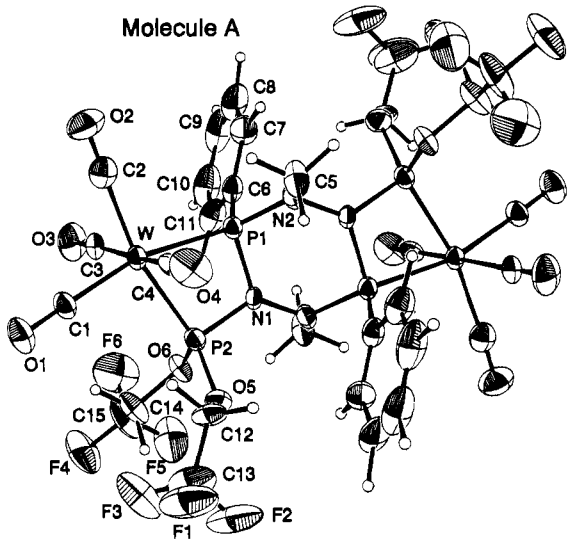

Figure 1. ORTEP representations of structures of 6. The thermal ellipsoids are drawn at the 50% probability level.

to $-PPh_2$ and >PPh groups respectively. The equivalence of both the sets of phosphane groups ($-PPh_2$ and >PPh) supports the bischelate structure with *cis* dispositions of the phosphane units around the metal centers in **2**. The ^{31}P NMR spectrum of **6** consisted of an $[AXR]_2$ (R = W) spin pattern, with one of the doublets centered at δ 94.0 ($^2J_{P-P}$ = 82.0 Hz), attributed to >PPh groups, and the other at δ 142.5, assigned to $P(OCH_2CF_3)_2$ groups. Two different W−P coupling values are observed in the ^{31}P NMR spectrum of **6**. Observation of a higher coupling value for $W-P(OCH_2CF_3)_2$ ($^1J_{W-P}$ = 312.0 Hz) as compared to W−PPh ($^1J_{W-P}$ = 258.0 Hz) units, clearly, indicated a strong tungsten−phosphorus interaction in the former presumably due to the better π-acceptor property of the phosphite groups.

The final confirmation of the four-membered metallacyclic structures proposed for **5** and **6** (Scheme 2) comes from an X-ray crystal structure analysis of a representative compound **6**. The ORTEP plot is shown in Figure 1, and the salient bonding parameters are summarized in Table 1. The structure comprises the neutral monomeric complex **6** with two crystallographically independent molecules in the asymmetric unit. The structure consists of W(0) centers bound to the >PPh and $-P(OCH_2CF_3)_2$ units in a *cis* fashion to afford the four-membered W(0)−P−N−P metallacycle. The strucutre is further characterized by a distorted octahedral geometry around W(0) and an acute angle (65.8(1)°) across the P1−W−P2 framework. A modest shortening of the W−P(2) bond (2.414(3) Å) as compared to W−P(1) (2.472(3) Å) may suggest a somewhat efficient π-back-bonding across the W−P(2) bond as a result of the presence of $-OCH_2CF_3$ groups on the P(2) center. The bisphosphorus hydrazide ring in **6** is in a *chair* confirmation and is identical to the *chair* conformations observed in a series of six-membered phosphorus hydrazide ring systems recently developed in our laboratory.[17]

Table 1. Selected Bond Lengths (Å) and Angles (deg) for Compound **6**

Wa−P1a	2.472(3)	Wb−P1b	2.457(3)
Wa−P2a	2.414(3)	Wb−P2b	2.419(3)
Wa−P2a	2.414(3)	Wb−C1b	1.995(13)
Wa−C2a	2.056(14)	Wb−C2b	2.036(12)
Wa−C3a	2.046(13)	Wb−C3b	2.007(12)
Wa−C4a	2.052(13)	Wb−C4b	1.986(11)
N1a−N2a[a]	1.431(12)	N1b−N2b[b]	1.454(11)
N2a−N1a[a]	1.431(12)	N2b−N1b[b]	1.454(11)
P2a−N1a	1.679(9)	P1b−N1b	1.713(9)
P1a−N1a	1.713(9)	P1b−N2b	1.666(9)
P1a−N2a	1.693(9)	P2b−N1b	1.676(8)
O1a−C1a	1.180(14)	O1b−C1b	1.145(15)
O2a−C2a	1.118(17)	O2b−C2b	1.150(15)
O3a−C3a	1.150(16)	O3b−C3b	1.147(15)
O4a−C4a	1.139(15)	O4b−C4b	1.140(14)
P1a−Wa−P2a	65.83(1)	P1b−Wb−P2b	65.88(10)
P1a−Wa−C1a	164.2(4)	P1b−Wb−C1b	98.9(4)
P1a−Wa−C2a	99.9(4)	P1b−Wb−C2b	90.7(3)
P1a−Wa−C3a	91.7(3)	P1b−Wb−C3b	94.1(4)
P1a−Wa−C4a	94.4(3)	P1b−Wb−C4b	166.2(4)
P2a−Wa−C1a	98.4(4)	P2b−Wb−C1b	164.8(4)
P2a−Wa−C2a	165.6(4)	P2b−Wb−C2b	91.7(4)
P2a−Wa−C3a	91.6(4)	P2b−Wb−C3b	91.6(4)
P2a−Wa−C4a	95.1(4)	P2b−Wb−C4b	100.5(4)
C1a−Wa−C2a	95.9(5)	C1b−Wb−C2b	88.2(5)
C1a−Wa−C3a	88.0(5)	C1b−Wb−C3b	89.6(5)
C1a−Wa−C4a	87.4(5)	C1b−Wb−C4b	94.7(5)
C2a−Wa−C3a	87.3(5)	C2b−Wb−C3b	175.0(5)
C2a−Wa−C4a	87.2(5)	C2b−Wb−C4b	87.8(5)
C3a−Wa−C4a	172.4(5)	C3b−Wb−C4b	87.9(5)
Wa−P1a−N1a	93.9(3)	Wb−P1b−C6b	121.3(4)
Wa−P1a−N2a	125.5(3)	N1b−P1b−N2b	104.6(4)
Wa−P1a−C6a	121.2(4)	Wb−P2b−N1b	96.5(3)
N1a−P1a−N2a	104.0(4)	P1b−N1b−N2b[b]	125.7(6)
N1a−P1a−C6a	107.2(5)	P2b−N1b−N2b[b]	131.3(7)
N2a−P1a−C6a	102.0(5)	P1b−N2b−N1b[b]	113.5(6)
Wa−P2a−O5a	126.8(3)	P1b−N2b−C5b	126.2(7)
Wa−P2a−O6a	124.6(3)	N1b[b]−N2b−C5b	118.2(8)
Wa−P2a−N1a	96.9(3)	Wb−C1b−O1b	176.0(11)
O5a−P2a−O6a	96.5(4)	Wb−C2b−O2b	179.4(11)
O5a−P2a−N1a	109.1(4)	Wb−C3b−O3b	179.4(11)
O6a−P2a−N1a	99.3(4)	Wb−C4b−O4b	178.0(12)
P1a−N1a−P2a	103.1(4)		
P1a−N1a−N2a[a]	127.2(7)		
P2a−N1a−N2a[a]	129.8(7)		
P1a−N2a−N1a[a]	112.5(7)		
P1a−N2a−C5a	123.8(8)		
N1a[a]−N2a−C5a	116.3(8)		
Wa−C1a−O1a	178.9(11)		
Wa−C2a−O2a	177.6(12)		
Wa−C3a−O3a	178.2(12)		
Wa−C4a−O4a	176.9(11)		

The new phosphorinane **4** reacts cleanly with $Pt(COD)Cl_2$ in dichloromethane to produce the bimetallic complex, $[\{PtCl_2\}_2\{\mu\text{-}[PhPN(Me)NP(OCH_2CF_3)_2]\}_2]$ (**7**) in 86% yield (Scheme 3). The chemical composition of **7** was established by C, H, and N analytical and multinuclear NMR spectroscopic data. The ^{31}P NMR spectrum of **7** consisted of two broad singlets at 83.7 ($^1J_{Pt-P}$ = 4172.0 Hz) and 87.0 ($^1J_{Pt-P}$ = 5552.0 Hz) ppm,

attributed to the >PPh and $-P(OCH_2CF_3)_2$ groups respectively. As expected, two different $^1J_{Pt-P}$ values are observed in the ^{31}P NMR spectrum. The presence of electronically demanding substituents (*i.e.*, OCH_2CF_3) on the exocyclic phosphorus in **4** is expected to generate stronger Pt−P interactions. An increase of 1380 Hz in the magnitude of $^1J_{Pt-P}$ on going from PhP−Pt to $(CF_3CH_2O)_2P-Pt$ in **4** may explain the influence of substituent electronic effects on the phosphane-metal bonding interactions.

Conclusions

A significant outcome of this investigation is concerned with the observed preference for the four-membered >P−N(R)−P< coordination rather than the normally favored five-membered >P−N(R)−N(R)−P< coordination. This unique preference for the four-membered M−P−N−P over the five-membered M−P−N−N−P coordination may be rationalized in terms of the electronic effects. The disposition of the lone pairs on P_A and P_B in an axial fashion is essential for P_A and P_B to coordinate with the metal across the $>P_A-N(R)-N(R)-P_B<$ framework. However, our recent detailed X-ray structural investigations of cyclic phosphorus(III) hydrazides (of the type present in **2** and **3**) clearly suggested equatorial dispositions of the lone pairs on the ring P(III) centers.[17] Therefore, the metal is forced to interact with the equatorial lone pair of P_A and P_C to give a four-membered metallacycle as outlined in Scheme 2. It may be conceived that the energy involved for the equatorial to axial flip of the lone pair of P_A, to produce a five-membered $>P_A-N-N-P_B-M$ metallacycle, is presumably much more than the strain involved in a less favored four-membered $>P_A-N-P_C-M$ metallacycle in **6**.

Experimental Section

Materials. All reactions were carried out under purified nitrogen by standard Schlenk techniques. Solvents were purified and dried by standard methods and distilled under nitrogen prior to use. Reagents such as $PPhCl_2$, PCl_3, CF_3CH_2OH, *cis*-$Pt(COD)Cl_2$, and *cis*-$[Mo(CO)_4(NHC_5H_{10})_2]$ were purchased from Aldrich Chemical Co. and were used without further purification. $[W(CO)_4(NHC_5H_{10})_2]$ was prepared by literature methods.[21] Triethylamine was distilled over KOH and stored over molecular sieves under N_2. $[PhPN(Me)N(H)]_2$ (**1**) was prepared by the reaction of methyl hydrazine and $PhPCl_2$, as reported earlier.[17]

Nuclear magnetic resonance spectra were recorded on Bruker ARX-300 spectrometer using $CDCl_3$ solvent. The ^1H NMR chemical shifts are reported in ppm, downfield from external standard $SiMe_4$. The ^{31}P NMR spectra were recorded with 85% H_3PO_4 as an external standard and positive chemical shifts lie downfield of the standard. Infrared spectra were recorded using Nujol mulls on a Mattson Galaxy 3000 spectrophotometer. Elemental analyses were performed by Oneida Research Services, Inc., New York.

$[PhPN(Me)N(PPh_2)]_2$ (2). A solution of PPh_2Cl (7.26 g, 32.90 mol) in chloroform (50 mL) was added dropwise to a solution of **1** (5.0 g, 16.45 mmol) and Et_3N (3.43 g, 34.0 mmol) in chloroform (200 mL) at 25 °C with constant stirring. The reaction mixture was stirred at 25 °C for 12 h under a stream of dry nitrogen. The solvent was completely removed *in vacuo*, and the resulting white residue was washed with water to remove $Et_3N{\cdot}HCl$, then with hexane and dried *in vacuo* to obtain the compound **2** as white powder in 84% (9.3 g) yield. mp: 215 °C. Anal. Calcd for $C_{38}H_{36}N_4P_4$: C, 67.8; H, 5.4; N, 8.3. Found: C, 66.8; H, 5.8; N, 8.7. ^1H NMR: δ 3.37 (d, $^3J_{P-H}$ = 13.7 Hz, 6H, NCH_3), 6.5−7.8 (m, 30H, Ph). ^{31}P NMR: δ 64.6 (d, $^2J_{P-P}$ = 31.2 Hz, PPh_2), 106.2 (d, $^2J_{P-P}$ = 31.2 Hz, *P*Ph).

$[PhPN(Me)N\{P(OCH_2CF_3)_2\}]_2$ (4). A solution of PCl_3 (4.52 g, 32.90 mol) in chloroform (50 mL) was added dropwise to a solution of **1** (5.0 g, 16.45 mmol) and Et_3N (3.43 g, 34.0 mmol) in chloroform (200 mL) at 25 °C with constant stirring. The reaction mixture was stirred at 25 °C till the formation of the compound **3** was complete (2h, ^{31}P NMR: δ 87.4 (d, $^2J_{P-P}$ = 40.0 Hz, *P*Ph), 163.7 (d, $^2J_{P-P}$ = 40.0 Hz, PCl_2)). The solution was concentrated to ~50 mL *in vacuo*. To the resulting solution, was added an hexane (200 mL) solution of trifluoroethanol (3.32 g, 33.2 mmol) and Et_3N (3.43 g, 34.0 mmol) at 25 °C with constant stirring. The reaction mixture was further stirred for 2 h and then refluxed for 1 h before filtering off the $Et_3N{\cdot}HCl$. Removal of the solvent *in vacuo* gave compound **4** as a white crystalline solid in 64% (8.0 g) yield. Mp: 96 °C. Anal. Calcd for $C_{22}H_{24}N_4P_4O_4F_{12}$: C, 34.7; H, 3.2; N, 7.4%. Found: C, 34.2; H, 3.5; N, 7.6%. ^1H NMR: δ 3.15 (d, $^3J_{P-H}$ = 16.9 Hz, 6H, N-CH_3), 4.2 (m, 8H, OCH_2), 7.2−7.9 (m, 10H, Ph). ^{31}P NMR: δ 85.1 (d, $^2J_{P-P}$ = 37.0 Hz, *P*Ph), 147.5 (d, $^2J_{P-P}$ = 37.0 Hz, $P(OCH_2CF_3)_2$).

$[\{Mo(CO)_4\}_2\{\mu\text{-}[PhPN(Me)N(PPh_2)]_2]$ (5). A solution of *cis*-$[Mo(CO)_4(NHC_5H_{10})_2]$ (0.40 g, 0.859 mmol) in dichloromethane (25 mL) was added dropwise at 25 °C to a solution of **2** (0.356 g, 0.429 mmol) also in dichloromethane (25 mL). The reaction mixture was heated under reflux for 4 h before the solvent was removed *in vacuo* to obtain a pale yellow microcrystalline powder. This residue was extracted from a mixture of dichloromethane/hexane (3:1 ratio) and the extracts (2 × 20 mL) were filtered through a column of silica gel (20 gm). Evaporation of the solvent *in vacuo* gave complex **5** in 72% (0.41 g) yield. Mp: 238 °C dec. Anal. Calcd for $C_{46}H_{36}N_4O_8P_4Mo_2$. C, 50.6; H, 3.3; N, 5.1. Found: C, 49.9; H, 3.4; N, 5.1. IR Nujol (ν(CO)): 2022 (sh), 1954 (s), 1923 (m), 1894 (vs) cm^{-1}. ^1H NMR: δ 3.16 (d, $^3J_{P-H}$ = 12.6 Hz, 6H, NCH_3), 6.6−7.8 (m, 30H, Ph). ^{31}P NMR: δ 97.4 (d, $^2J_{P-P}$ = 45.0 Hz, PPh_2), 121.0 (d, $^2J_{P-P}$ = 45.0 Hz, *P*Ph).

$[\{W(CO)_4\}_2\{\mu\text{-}[PhPN(Me)N(P(OCH_2CF_3)_2)]_2]$ (6). A solution of *cis*-$[W(CO)_4(NHC_5H_{10})_2]$ (0.40 g, 0.859 mmol) in dichloromethane (25 mL) was added dropwise at 25 °C to a solution of **2** (0.33 g, 0.429 mmol) also in dichloromethane (25 mL). The reaction mixture was heated under reflux for 4 h and worked up as described above for **5**, to obtain a pale yellow microcrystalline powder. The resulting product was recrystallized from dichloromethane/hexane (2:1 v/v) to obtain analytically pure compound **6** in 65% (0.40 g) Mp: 202 °C dec. Anal. Calcd for $C_{30}H_{24}F_{12}N_4O_{12}P_4W_2{\cdot}CH_2Cl_2$: C, 25.9; H, 1.8; N, 3.9. Found: C, 25.6; H, 1.7; N, 3.8. IR Nujol (ν(CO)): 2037 (sh), 1975 (s), 1956 (m), 1925 (vs) cm^{-1}. ^1H NMR: δ 3.52 (d, 6H, NCH_3), 4.2 (m, 8H, NCH_2), 7.4−7.8 (m, 10H, Ph). ^{31}P NMR: δ 94.0 (d, $^2J_{P-P}$ = 82.0 Hz, $^1J_{W-P}$ = 262.0 Hz, PPh), 142.5 (d, $^2J_{P-P}$ = 82.0 Hz, $^1J_{W-P}$ = 312.0 Hz, $P(OCH_2CF_3)_2$).

$[\{PtCl_2\}_2\{\mu\text{-}[PhPN(Me)N(P(OCH_2CF_3)_2)]_2]$ (7). A dichloromethane (20 mL) solution of **4** (0.105 g, 0.395 mmol) was added dropwise at 25 °C to a solution of $[PtCl_2(COD)]$ (0.40 g, 0.785 mmol) also in dichloromethane (25 mL). The reaction mixture was stirred for 2 h. Addition of hexane (25 mL) to the resulting solution gave a precipitate which was filtered and dried *in vacuo* to obtain compound **7** in 76% (0.27 g) yield. Mp: >250 °C. Anal. Calcd for $C_{22}H_{24}Cl_4F_{12}N_4P_4O_4Pt_2$: C, 20.5; H, 1.9; N, 4.4. Found: C, 21.3; H, 1.7; N, 4.8. ^1H NMR: δ 3.75 (d, $^3J_{P-H}$ = 13.2 Hz, 6H, NCH_3), 4.2 (m, 8H, OCH_2), 7.2−7.9 (m, 10H, Ph). ^{31}P NMR: δ 83.7 (s, br, $^1J_{Pt-P}$ = 4172.0 Hz, *P*Ph), 87.0 (s, br, $^1J_{Pt-P}$ = 5552.2 Hz, $P(OCH_2CF_3)_2$).

X-ray Data Collection and Processing. The crystal data and details of data collection for **6** are given in Table 2. Pale yellow crystals of **6** suitable for X-ray diffraction were obtained from dichloromethane/

Table 2. Crystal Data for Complex **6**

formula	$C_{30}H_{24}N_4O_{12}F_{12}P_4W_2{\cdot}CH_2Cl_2$	V, Å^3	2425.0(2)
		d_{calc}, g/cm^3	1.965
cryst system	triclinic	cryst size, mm	0.07 × 0.16 × 0.45
space group	$P\bar{1}$		
fw	1437.04	μ, mm^{-1}	5.07
a, Å	11.098(7)	no. of unique reflcns	4502
b, Å	11.263(6)	no. of rflcns with $I > 2$	3800
c, Å	20.107(8)		
α, deg	104.22(3)	no. of variables	605
β, deg	92.16(3)	R; R_w [a]	0.041; 0.054
γ, deg	94.38(3)	GOF	1.94
Z	2	max shift/σ	0.041
F(000)	1372	res. electron density	1.36 e/Å^3

[a] $R = \Sigma(|F_o| - |F_c|))/\Sigma(|F_o|)$, $R_w = [\Sigma w(|F_o| - |F_c|)^2/\Sigma w/(|F_o|)^2]^{1/2}$.

(21) Darensbourg, D. J.; Kemp, R. L. *Inorg. Chem.* **1978**, *17*, 2680.

Table 3. Final Fractional Atomic Coordinates and Equivalent Isotropic Displacement Coefficients (Å^2) for the Atoms of **6**

	x	y	z	B or B_{eq}		x	y	z	B or B_{eq}
Wa	0.24615(4)	0.10391(4)	0.11814(2)	3.43(2)	F2b	0.1461(12)	0.8767(13)	0.3210(7)	13.8(9)
P1a	0.3596(3)	0.0428(3)	0.01345(14)	3.28(14)	F3b	−0.0270(16)	0.9206(14)	0.3434(7)	17.6(12)
P2a	0.3732(3)	0.0606(3)	0.11850(15)	3.51(14)	F4b	0.2550(12)	1.0401(10)	0.5661(6)	12.7(8)
F1a	0.5758(12)	0.0816(11)	0.3443(5)	12.6(8)	F5b	0.3602(16)	1.0804(11)	0.4900(10)	19.6(13)
F2a	0.6129(12)	−0.0932(10)	0.2819(5)	12.7(8)	F6b	0.1825(17)	1.0390(11)	0.4749(9)	19.4(13)
F3a	0.4369(14)	−0.0612(14)	0.3120(6)	14.7(10)	O1b	0.3867(9)	0.2728(9)	0.3486(5)	6.8(5)
F4a	0.1514(11)	−0.4127(10)	0.1742(6)	12.4(8)	O2b	0.4846(8)	0.6373(9)	0.4928(5)	6.7(5)
F5a	0.2950(11)	−0.4500(9)	0.1017(7)	12.0(8)	O3b	0.0587(9)	0.4027(10)	0.2697(5)	7.5(6)
F6a	0.1343(11)	−0.3839(12)	0.0741(7)	14.0(9)	O4b	0.3941(9)	0.6406(10)	0.2812(5)	7.9(6)
O1a	0.1359(9)	0.1203(9)	0.2628(4)	6.7(5)	O5b	0.0343(8)	0.7380(9)	0.4021(4)	6.1(5)
O2a	0.1003(10)	0.3095(9)	0.0772(6)	8.2(6)	O6b	0.1926(8)	0.8056(7)	0.4909(5)	6.3(5)
O3a	0.0208(8)	−0.0886(10)	0.0525(6)	8.0(6)	N1b	0.0686(7)	0.6070(7)	0.4896(4)	2.9(4)
O4a	0.4414(10)	0.3215(9)	0.1953(5)	7.9(6)	N2b	0.0318(7)	0.3626(8)	0.4668(4)	3.2(4)
O5a	0.4783(7)	−0.0629(7)	0.1754(4)	4.6(4)	C1b	0.3453(11)	0.3651(12)	0.3621(6)	4.6(7)
O6a	0.3252(7)	−0.2027(7)	0.1039(4)	4.6(4)	C2b	0.4039(10)	0.5949(12)	0.4545(6)	4.6(6)
N1a	0.4356(7)	0.0619(8)	0.0436(4)	3.1(4)	C3b	0.1329(11)	0.4446(11)	0.3120(6)	4.6(6)
N2a	0.4705(8)	0.1316(8)	0.0113(5)	3.8(4)	C4b	0.3452(11)	0.5948(12)	0.3185(6)	4.7(6)
C1a	0.1768(11)	0.1155(11)	0.2090(6)	4.4(6)	C5b	0.0139(12)	0.2588(11)	0.4093(7)	5.5(7)
C2a	0.1514(12)	0.2382(12)	0.0931(7)	5.4(7)	C6b	0.2133(9)	0.4798(10)	0.5629(5)	3.1(5)
C3a	0.1017(11)	0.0184(12)	0.0752(7)	5.0(7)	C7b	0.2575(11)	0.5905(12)	0.6067(7)	5.3(7)
C4a	0.3743(11)	0.2417(12)	0.1672(6)	4.7(7)	C8b	0.3244(13)	0.5927(14)	0.6685(7)	6.7(8)
C5a	0.5067(13)	0.2607(11)	0.0251(8)	6.0(7)	C9b	0.3486(12)	0.4875(13)	0.6842(7)	5.9(7)
C6a	0.2828(10)	0.0387(11)	0.0686(6)	4.2(6)	C10b	0.3058(12)	0.3785(14)	0.6389(7)	6.2(8)
C7a	0.2628(12)	0.0238(14)	0.1187(6)	6.3(9)	C11b	0.2370(11)	0.3743(10)	0.5790(6)	4.3(6)
C8a	0.1892(14)	0.0300(22)	0.1757(8)	9.9(13)	C12b	0.0137(14)	0.7173(14)	0.3318(8)	6.8(9)
C9a	0.1405(14)	0.1499(19)	0.1865(8)	9.7(11)	C13b	0.0301(16)	0.8361(18)	0.3119(9)	8.8(11)
C10a	0.1578(13)	0.2127(16)	0.1373(9)	8.6(10)	C14b	0.2906(14)	0.8804(13)	0.4776(9)	7.7(9)
C11a	0.2283(12)	0.1568(14)	0.0771(7)	6.5(8)	C15b	0.2766(17)	1.0026(15)	0.5009(8)	8.6(10)
C12a	0.5125(13)	0.0398(12)	0.2321(6)	5.4(7)	Cl1	0.8143(13)	0.6622(13)	0.0682(7)	11.7(4)
C13a	0.5323(18)	0.0098(15)	0.2921(8)	9.1(10)	Cl2	0.5899(15)	0.5911(14)	0.1214(8)	13.5(4)
C14a	0.2649(14)	0.2448(13)	0.1568(7)	6.5(8)	Cl3	0.8329(18)	0.5468(18)	0.1768(10)	11.1(5)
C15a	0.2108(18)	0.3754(18)	0.1252(10)	10.4(12)	Cl4	0.6367(20)	0.6742(19)	0.1659(11)	12.6(6)
Wb	0.26234(4)	0.51978(4)	0.38605(2)	3.23(2)	Cl5	0.714(3)	0.555(3)	0.0551(19)	17.0(11)
P1b	0.1423(3)	0.4760(3)	0.47881(14)	2.99(13)	Cl6	0.7912(22)	0.4818(22)	0.1377(13)	11.3(6)
P2b	0.1384(3)	0.6817(3)	0.43735(16)	3.60(14)	CCl	0.751(5)	0.586(4)	0.121(3)	28.9(21)
F1b	−0.0001(11)	0.8212(12)	0.2457(5)	11.9(8)					

hexane (2:1 v/v) at 0 °C, with CH_2Cl_2 as solvate molecule. All X-ray data were collected on an Enraf-Nonius CAD-4 diffractormeter with Mo Kα radiation and a graphite monochromator at 22(1) °C. The unit cell dimensions were obtained from a least squares fit to setting angles of 25 reflections. The crystal did not exhibit any significant decay under X-ray irradiation.

The structures were solved by direct methods and were subsequently refined by full-matrix least square method which minimizes $\Sigma w/(|F_o| - |F_c|)^2)$ where $w^{-1} = [\sigma(\text{counting}) + (0.008(F_o)^2)/4F_o]$. Atomic scattering factors which included anomalous scattering contributions were from ref 22. All hydrogen atoms in both the structures were located in difference Fourier maps and refined with the fixed isotropic thermal parameters. The final cycle of the least-squares refinement gave an agreement factor R of 0.041. The final positional parameters and their equivalent thermal parameters for all non hydrogen atoms are listed in Table 3. The programs used for the crystallographic computations are reported in ref 23. Listings of full experimental details, coordinates, temperature factors, and anisotropic temperature factors are deposited as supplementary material.

(22) *International Tables For X-ray Crystallography*, Kynoch Press: Birmingham, England, 1974; Vol. 4.

Acknowledgment. This work was supported by funds provided by DOE Grant DEFG0289E R60875 and by the Departments of Chemistry, Radiology and Research Reactor, University of Missouri. Partial funding of the X-ray diffractometer by the National Science Foundation, Grant No. CHE-[90-11804], is gratefully acknowledged.

Supplementary Material Available: Tables of bond distances and angles, H atom coordinates, and thermal parameters for **6** (14 pages). Ordering information is given on any current masthead page.

IC940890H

(23) The following references are relevant to the NRCVAX system: (a) Gabe, E. J.; Page, Y. L.; Charland, J. L.; Lee, F. L.; White, P. S. *J. Appl. Crystallogr.* **1989**, *22*, 384. (b) Flack, L. *Acta Crystallogr. Sect. A*, **1983**, *39*, 876. (c) Johnson, C. K. *ORTEP- A Fortran Thermal Ellipsoid Plot Program*; Technical Report ORNL-5138; Oak Ridge National Laboratories: Oak Ridge, TN, 1976. (d) Larson, A. C. *Crystallographic Computing*; Munksgaard: Copenhagen, 1970; p 293. (e) Page, Y. L. *J. Appl. Crystallogr.* **1988**, *21*, 983. (f) Page, Y. L.; Gabe, E. J. *J. Appl. Crystallogr.* **1979**, *12*, 464. (g) Rogers, D. *Acta Crystallogr., Sect. A*, **1981**, *37*, 7.